

Formation of Carbonaceous Materials by Ultrasonic Atomization of Aqueous Ethanol Solution and Pyrolysis Treatment

Osamu Terakado,^{1,*} Genki Yamane¹ and Masahiro Hirasawa¹

¹ Department of Materials Science and Engineering, Graduate School of Engineering, Nagoya University, Nagoya, Japan

Abstract. The ultrasonic atomization of aqueous ethanol solution and the consequent pyrolysis treatment has been employed in order to explore a new technique for preparation of carbonaceous compounds. The deposition of fibrous carbon on titanium catalyst has been observed after 5 hours of treatment at pyrolysis temperature of 973–1173 K. The yield in carbon has increased in comparison to the control experiment without ultrasonic atomization. A TEM analysis has shown that the fibre has the diameter of ~ 30 nm and the fibre growth occurs from the catalyst particles.

Keywords. Ultrasound, atomization, pyrolysis, carbon, ethanol.

PACS®(2010). 43.35.+d, 81.05.U-, 81.15.Gh.

1 Introduction

Irradiation of ultrasound from bulk liquid towards the liquid-gas interface causes a capillary fountain jet. Ultrasonic atomization is a phenomenon in which liquid droplets are generated from the fountain jet. The mist size is related with the dimension of the corresponding capillary wave, and the droplet size, d , is given by:

$$d = k(8\pi\sigma/\rho f^2)^{1/3}, \quad (1)$$

where σ and ρ are surface tension and density of the liquid, respectively, f is frequency of the applied ultrasound, and the constant k is around 0.3 [1]. Thus, the droplet size is of the order of micron-meter, when an ultrasound with the frequency of a few MHz is applied.

Corresponding author: Osamu Terakado, Department of Materials Science and Engineering, Graduate School of Engineering, Nagoya University, Furo-cho, Chikusa-ku, 464-8603 Nagoya, Japan; E-mail: teramon@numse.nagoya-u.ac.jp.

Received: January 31, 2011. Accepted: April 15, 2011.

One of the interesting applications of the ultrasonic atomization technique is the separation of ethanol from aqueous ethanol solution. Sato et al. found that the ethanol concentration in mist phase was significantly higher than that of the bulk liquid [2]. Recent studies on small X-ray scattering and scanning mobility particle sizer measurements revealed that two groups of the mist droplets were formed in the ultrasonic atomization of aqueous ethanol solution: one was the micrometer-sized droplet, as evaluated by eq. (1), and the other nanosized droplets [3, 4]. The latter, formed by the acoustic excitation of the ethanol-rich gas-liquid interface due to the hydrophobic property of ethyl group in the ethanol molecule, is responsible for the condensation of the ethanol in the mist phase.

Pyrolysis treatment of droplets produced by ultrasonic atomization, or ultrasonic spray pyrolysis is successfully applied in production of various materials, with significant stress on the production of ceramics materials [5]. However, less is known about the carbonization behaviour of mists produced by ultrasonic atomization of aqueous ethanol solution. An optimisation of the experimental conditions can lead to the establishment of a production process of useful carbon materials. Moreover, this method can be applied for the removal of hydrophobic organic contaminants in wastewater, and the consequent fixation as solid carbon. In the present paper we report the carbonization behaviour of mists, produced by ultrasonic atomization of aqueous ethanol solution, at catalyst surface.

2 Experimental Procedure

Figure 1 shows the schematic experimental set-up of the ultrasonic spray pyrolysis. Aqueous ethanol solution (250 mL), prepared by dissolution of ethanol (99.5%, Wako pure chemical) into distilled water, was fed into a container made of acrylic resin or pyrex glass (inner diameter = 80 mm, height = 150 mm). In this paper, the results of the composition of 80 mass% of ethanol are presented, though it has been found that there is essentially no composition dependence on the formation of the carbonaceous compounds obtained by this technique.

The sample solution was atomized by piezoelectric transducer (HM-1630 unit, Honda electric) which was connected at the bottom of the container. The operating frequency was 1.6 MHz, and the electric input was 30 W. The mist was introduced by argon carrier gas into quartz glass

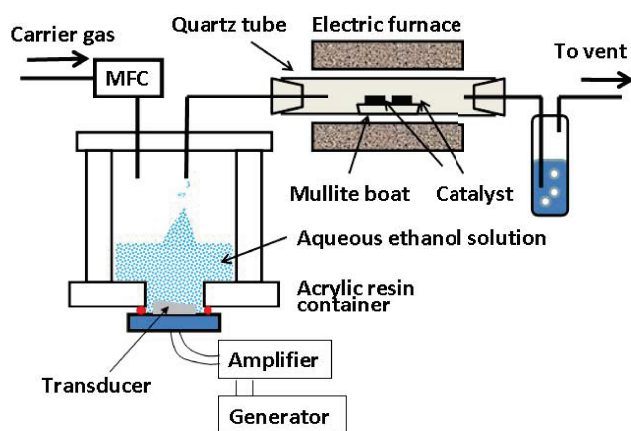


Figure 1. Schematic experimental set-up for ultrasonic atomization and pyrolysis treatment.

reactor (i.d. 26 mm, length of 600 mm) which was heated at 973–1173 K by an electric furnace. We examined iron, nickel, molybdenum, and titanium plate as catalysis for the carbon deposition. The catalysis plate was put on a mullite boat which is put in the middle of the reactor. The sample mist was introduced for 5 hours with the argon flow rate of 100 mL/min. As a control experiment, we carried out also a pyrolysis where the ultrasound was not irradiated and the carrier gas was introduced over the ethanol solution at room temperature into the reactor. After the pyrolysis run, the carbon deposited on the catalysis was collected carefully and characterized by SEM (JSM-6060, JOEL), Raman spectroscopy (NRS-1000, JASCO) and TEM (H-800, Hitachi).

3 Results and Discussion

3.1 Formation of Carbonaceous Compounds on Catalyst Surface

Figure 2 shows the photographs of titanium and iron catalysts after 5 hours of ultrasonic atomization – pyrolysis treatment. The deposition of black powder is observed on the catalyst surface of titanium and iron. On the other hand, such a deposition is not clearly visible for nickel and molybdenum, and the samples of control experiment without irradiation of ultrasound. Thus, the appropriate selection of catalyst and the application of ultrasound are necessary for the formation of carbonaceous compounds. The increase in the amount of deposition is presumably due to the increase in ethanol in unit volume arising from the atomization.

As for the yield of carbonaceous compounds, the mass of catalyst increased after the treatment by ~ 10 mg at 973 K and ~ 110 mg at 1173 K in the case of titanium catalyst. In the present study, however, further quantitative discussion on the yield of carbon is not held, because mass increase due to the oxidation of the catalyst surface should be

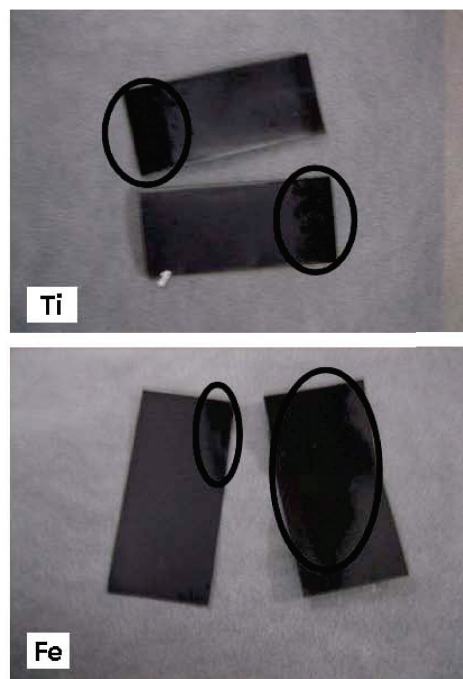


Figure 2. Photographs of titanium and iron catalyst after the atomization – pyrolysis treatment at 973 K for 5 hours. The colour of metal surface changed to black in the encircled area.

also considered, as will be mentioned in the following sections. Furthermore, most of ethanol molecules in gas phase or mist phase flow apart from the catalyst surface. It should be noted that the width of the catalyst is one third of the inner diameter of the quartz reactor and that the gas or mist flows parallel to the catalyst on the mullite boat. The total

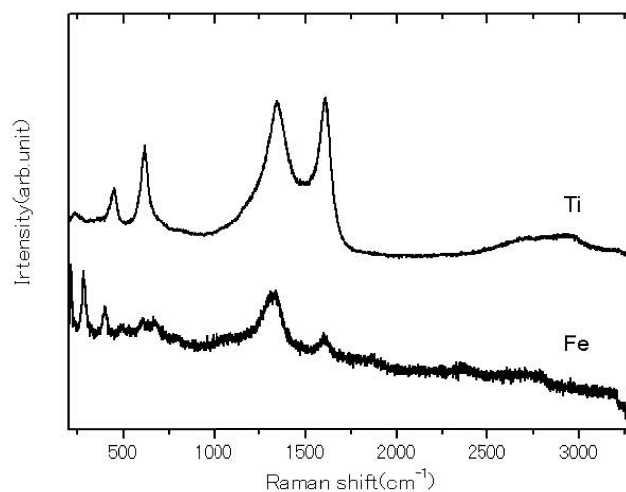


Figure 3. Raman spectra of Ti and Fe catalyst surface. The experimental condition of the treatment is the same as those in Figure 2. The pyrolysis temperature is 973 K.

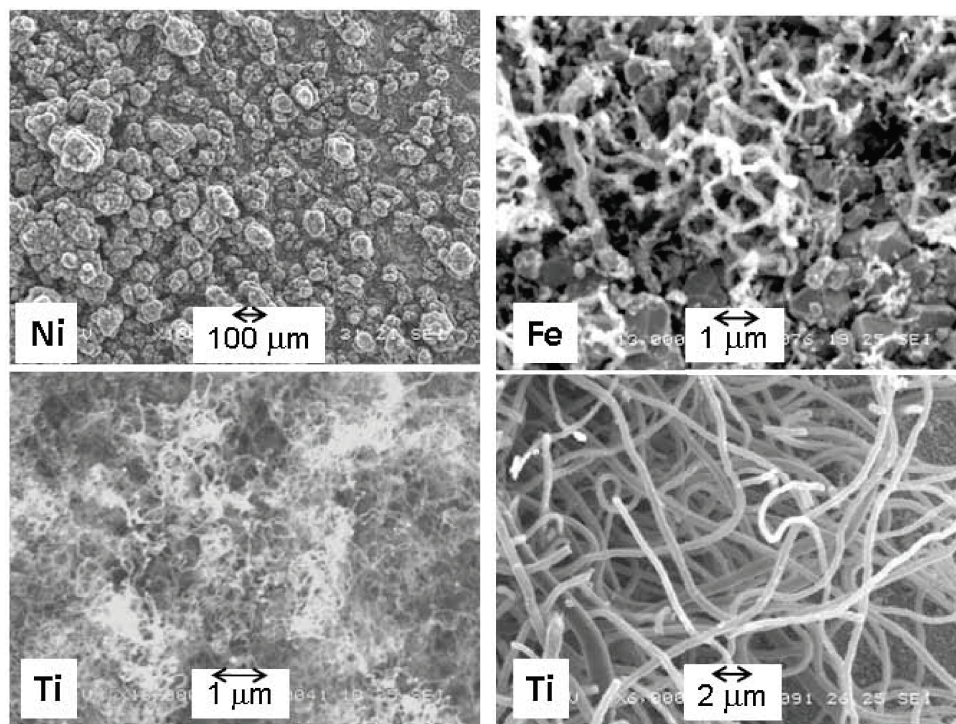


Figure 4. SEM images of the Ni, Fe, and Ti catalyst surface. The pyrolysis temperature is 973 K.

yield depends strongly on the flow pattern of the gas or mist around the catalyst. Further work is needed with respect to this point.

3.2 Raman Spectroscopy Measurement of Deposits

For the characterization of carbonaceous deposits we have carried out Raman spectroscopy measurements of the deposits with the catalyst. Figure 3 shows the spectra of titanium and iron. Raman peaks at wavenumber of ~ 1580 and 1360 cm^{-1} ($1\text{ cm}^{-1} = 100\text{ m}^{-1}$) are observed in all the spectra. These peaks are known as G or Graphite band for the former and D or Disorder band for the latter, respectively. The former is due to the sp^2 structure of the graphite, while the latter arises from the structural disorder of the perfect graphite. In order to discuss the crystallinity of the carbonaceous compounds, the *R*-value, ratio of the intensity of D band and that of G band is employed [6]. In all the cases the *R*-value is found to be more than 0.9. It is known that a carbonaceous material has the crystallinity very similar to that of natural graphite in case of $R < 0.2$ [6]. The present result indicates that the carbonaceous compounds obtained in this method do not have high crystallinity.

As seen in Figure 3, relative peak intensity of G and D bands in the case of iron catalyst is weaker than that of titanium, suggesting that the relative amount of carbonaceous compounds is less. This is in accordance with the SEM observation of iron surface (see Section 3.3). In addition, Raman peaks around 210 , 280 and 400 cm^{-1} are observed

that can be attributed to those of Fe_2O_3 [7]. The oxidation of iron takes place during the treatment. For the results of Ti catalyst, Raman peaks around 450 and 600 cm^{-1} are observed that are attributed to those of rutile form of TiO_2 [8].

3.3 SEM Observation

The SEM image of the carbonaceous compounds deposited on the catalyst is shown in Figure 4. The fibrous materials with the diameter of less than $1\text{ }\mu\text{m}$ are clearly observed on the titanium catalyst surface. On the other hand, essentially no deposition of carbonaceous compounds has been observed on nickel surface. In the case of iron catalyst, slight amount of fibrous materials are observed, though the main materials are particulates, presumably iron oxides. Thus, the oxidation prevails for the nickel and iron catalysts in the present experimental conditions. It should be noted that the introduction of reducing agent such as hydrogen is essential in the production of carbon fibers or nanotubes by chemical vapor deposition, CVD, on metal catalysts.

3.4 TEM Analysis

We have further performed TEM analysis in order to characterize the carbonaceous materials. Figure 5 shows the TEM image of materials deposited on titanium and the corresponding electron diffraction pattern. It is clearly seen that fibrous carbonaceous compounds have the diameter of $\sim 30\text{ nm}$ and that they exhibit the diffraction peak which is

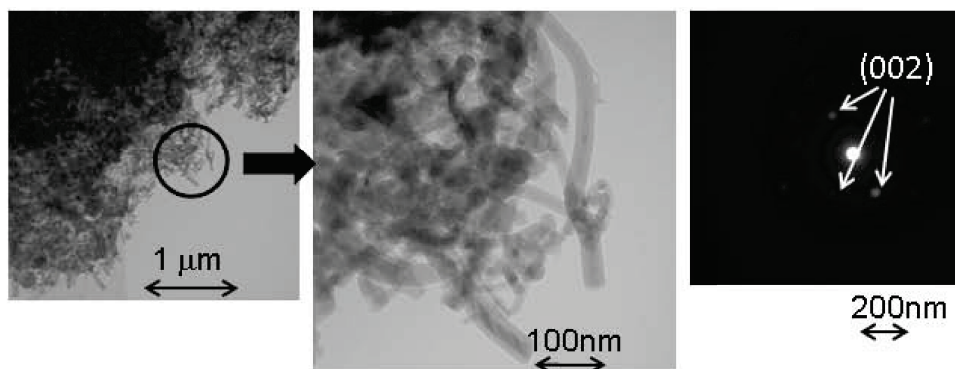


Figure 5. TEM images of the carbonaceous compounds formed on the titanium catalyst. (Left) Overview of the image, (Middle) Image of the circle in the left image with higher resolution, (Right) Electron diffraction pattern obtained from the middle TEM image. The pyrolysis temperature is 1023 K.

coincident to that of (002) diffraction of graphite. Furthermore, the fiber grows from the crystalline particles, as indicated by arrows in Figure 6. The energy dispersion spectra showed that the particles are obviously titanium. In the present study detailed mechanism of the carbon formation is not clear. It is expected that the evaporation of mists occur rather drastically inside the pyrolysis reactor and the concentrated ethanol vapor decomposes at catalyst surface. Therefore, an analogy can be made in the formation of carbon nanofibers in CVD technique [9]. In this case, vapor of carbon source decompose at the catalyst surface and the carbon is dissolved in metal to form intermediate carbides. Further supply of carbon source leads to the deposition of carbon around the catalyst surface and the metal particle is squeezed out because of the liquid-like behaviour of metal in contrast to firm graphite layers [9]. The fresh metal surface is, then, exposed to the gas phase, and further process can result in pulsed or lump-formed growth of carbon fibers.

Such a vapor-liquid-solid mechanism can be responsible for the growth of carbon fibers.

As for the difference in the carbon yield among catalysts, surface oxidation and the stability of carbide should be considered. Iron and nickel are well known catalysts for the carbon fibers and nanotubes [9]. Few yields of carbon deposits in case of iron and fewer for nickel can be understood by the surface oxidation, as mentioned in Section 3.2. Higher carbon yield in the case of titanium catalyst can be ascribed to the higher stability of carbide in comparison to those of iron and nickel. Any trace of titanium carbide has not been, so far, observed in TEM observation, though this can be due to the phase change after cooling down the sample. Further studies are needed in order to clarify the detailed growth mechanism.

In summary, the application of ultrasonic atomization is effective in the view of the significant increase in the amount of carbon. Further optimization of experimental parameters, such as precise control of pyrolysis atmosphere, is needed to increase further the carbon yield as well as to control their phase.

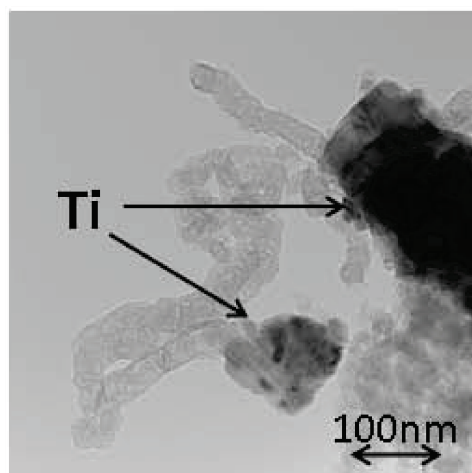


Figure 6. TEM image of the carbonaceous compounds with titanium particles. The pyrolysis temperature is 1023 K.

4 Conclusion

In the present paper we have addressed the carbonization of aqueous ethanol solution atomized by ultrasound. The atomization leads to substantial increase in carbon yield. In the present experimental condition, titanium catalyst is the most effective in the amount of carbon. The fibrous materials have the diameter of ~ 30 nm, and the growth from the titanium particles has been observed.

As mentioned in introduction, ultrasonic atomization process enables the removal of hydrophobic organic compounds from industrial wastewater. An example is wastewater discharged from cokes oven in steel industry, that is normally high load of chemical oxygen demand (COD) compounds. As for the effective usage of recovered organic compounds, carbonization is one of the promising methods

to fix the carbon resources. The optimization of the process parameters can lead to the establishment of an effective wastewater treatment.

Acknowledgments

The authors acknowledge Dr. Shigeo Arai (Eco Topia Science Institute, Nagoya Univ.) for his kind support in TEM measurements. Financial support by Steel Industry Foundation for the Advancement of Environmental Protection Technology, Japan is gratefully acknowledged.

References

- [1] R. J. Lang, Ultrasonic atomization of liquids, *J. Acoust. Soc. Am.*, **25** (1962), 6.
- [2] M. Sato, K. Matsuura and T. Fujii, Ethanol separation from ethanol-water solution by ultrasonic atomization and its proposed mechanism based on parametric decay instability of capillary wave, *J. Chem. Phys.*, **114** (2001), 2382.
- [3] Y. F. Yano, K. Matsuura, T. Fukazu, F. Abe, A. Wakisaka, H. Kobara, K. Kaneko, A. Kumagai, Y. Katsuya and M. Tanaka, Small-angle x-ray scattering measurement of a mist of ethanol nanodroplets: An approach to understanding ultrasonic separation of ethanol-water mixtures, *J. Chem. Phys.*, **127** (2007), 031101.
- [4] H. Kobara, M. Tamiya, A. Wakisaka, T. Fukazu and K. Matsuura, Relationship between the size of mist droplets and ethanol condensation efficiency at ultrasonic atomization on ethanol-water mixtures, *AIChE J.*, **56** (2010), 810.
- [5] P. S. Patil, Versatility of chemical spray pyrolysis technique, *Mater. Chem. Phys.*, **59** (1999), 185.
- [6] The Carbon Society of Japan, *The most up-to-date experimental techniques for the physical characterization of carbonaceous materials*, Realize Science & Engineering, Tokyo, (2001) 89. (In Japanese)
- [7] O. N. Shebanova and P. Lazor, Raman study of magnetite (Fe_2O_3): laser-induced thermal effects and oxidation, *J. Raman Spec.*, **34** (2003), 845.
- [8] S. P. S. Porto, P. A. Fluery and T. C. Damen, Raman spectra of TiO_2 , MgF_2 , ZnF_2 , FeF_2 , and MnF_2 *Phys. Rev.*, **154** (1967), 522.
- [9] K. P. De Jong and J. W. Geus, Carbon nanofibers: catalytic synthesis and applications, *Catal. Rev. Sci. Eng.*, **42** (2000), 481.